

# Min-Proteins Oscillations in *E. coli*: Three-Dimensional Off-Lattice Stochastic Reaction-Diffusion Model

Vladimir Krstić,<sup>1</sup> Željka Maglica,<sup>2</sup> Hana Čipčić Paljetak,<sup>3</sup> Boris Podobnik<sup>4</sup> and Nenad Pavin<sup>1</sup>

Received January 31, 2006; accepted July 26, 2006

Published Online: September 12, 2006

---

The position of a division site in the rod-shaped bacterium *E. coli* is partially determined by pole-to-pole oscillations of the Min-family of proteins—MinC, MinD, and MinE. Furthermore, experiments reveal that MinD protein polymerizes on the membrane into filaments and that MinE protein forms an oscillating ring. We assume that MinD filaments are single-stranded (two-stranded hypothesis has been already tested in our previous paper [20]). In the filamentous cells zebra-striped MinD oscillation pattern, fully formed oscillating MinE rings, and weakly fluorescent, rapidly moving MinE rings are experimentally observed. All these phenomena are reproduced by our three-dimensional off-lattice stochastic reaction-diffusion model. An algorithm with adaptive time steps is implemented in order to speed up the time-consuming process of tracking each protein in the computer simulation.

---

**KEY WORDS:** off-lattice, stochastic, reaction-diffusion, MinD oscillations, MinE ring, *Escherichia coli*

---

## 1. INTRODUCTION

A division site in the rod-shaped bacterium *E. coli* is determined by the position of the ring of FtsZ protein formed on the inner layer of the cytoplasmic membrane.<sup>(1)</sup> The position of this ring is regulated by two mechanisms: nucleoid occlusion and the oscillations of the Min family of proteins, namely MinC, MinD, and MinE.<sup>(2)</sup>

---

<sup>1</sup> Department of Physics, Faculty of Science, University of Zagreb, Zagreb, Croatia; e-mail: vkrstic@phy.hr, npavin@phy.hr.

<sup>2</sup> ETH Zürich, Institute of Molecular Biology and Biophysics, CH-8093 Zürich, Switzerland.

<sup>3</sup> PLIVA Research Institute Ltd., Zagreb, Croatia.

<sup>4</sup> Faculty of Civil Engineering, University of Rijeka, Rijeka, Croatia; Zagreb School of Economics and Management, Zagreb, Croatia.

Both mechanisms inhibit the polymerization of FtsZ protein on the membrane. Nucleoid occlusion prevents formation of the FtsZ ring over the nucleoids, while pole-to-pole Min oscillations exclude the cell poles as a potential division site<sup>(3,4)</sup> (in the absence of Min-proteins, FtsZ ring may be formed near the cell poles resulting in cells lacking in the genetic material—minicells; hence the name Min).

Only MinD and MinE proteins are necessary for generating pole-to-pole Min oscillations.<sup>(5)</sup> However, the polymerization of FtsZ protein on the membrane is inhibited by the membrane-associated MinC protein.<sup>(6)</sup> Since this protein is recruited to the membrane by the membrane-associated MinD, MinD and MinC oscillation patterns are similar.<sup>(7)</sup>

Min oscillations are driven by ATP hydrolysis.<sup>(8)</sup> MinD protein only in its ATP bound form (MinD:ATP) can attach to the membrane. ATP hydrolysis stimulates the detachment of this protein from the membrane. However, MinD protein has low ATPase activity and, with no MinE present, it binds to the membrane and resides there thereafter—there are no oscillations. MinE attaches to the membrane-associated MinD and stimulates ATP hydrolysis: MinD:ADP, MinE, and phosphate are released into the cytoplasm. The released MinD:ADP cannot bind to the membrane until a nucleotide exchange converts MinD:ADP back into MinD:ATP.<sup>(8)</sup>

MinD and MinE oscillation patterns differ.<sup>(9)</sup> The membrane-associated MinD:ATP molecules form the polar cap, while the membrane-associated MinE molecules (in the MinE-MinD:ATP complex) form the ring (the MinE ring) at the beginning of the MinD polar cap. As the MinE ring moves toward the pole of the *E. coli*, the polar cap shrinks and starts to form at the opposite pole. At the time when the MinE ring reaches the pole, the old MinD polar zone is almost disassembled. Since at this pole there are few membrane-associated MinD:ATP molecules, the MinE ring disappears and reappears near the center of the bacterium at the beginning of the new MinD polar cap. The time-averaged distributions of the membrane-associated MinD and MinC proteins (MinC protein is recruited to the membrane by MinD) have the minimum at the middle of the cell. Since MinC protein inhibits polymerization of FtsZ, the middle of the cell is the most probable site for FtsZ ring formation.

MinD protein polymerizes on the membrane into filaments. An *in vitro* experiment suggests that these filaments are two-stranded.<sup>(10)</sup> However, there is no *in vitro* evidence to support this result.

MinD/MinE dynamical structures has been explored with the several analytical<sup>(11–17)</sup> and stochastic models.<sup>(18–21)</sup> Our three-dimensional off-lattice stochastic reaction-diffusion model<sup>(20)</sup> extends the previous ones by taking into account spatial organization of MinD/MinE on the membrane at the level of a single molecule. In that model, it has been assumed that MinD protein polymerizes on the membrane into two-stranded filaments. Since there is no *in vivo* experiment to support this assumption, it is important to study Min protein dynamics by using single-stranded MinD filaments.

## 2. THE MODEL AND SIMULATIONS

Huang *et al.*<sup>(14)</sup> proposed a model for Min oscillations based only on *in vitro* observed interactions of MinD and MinE proteins: (1) cytoplasmic MinD:ATP protein attaches to the membrane, (2) cytoplasmic MinE attaches to the membrane-associated MinD:ATP protein, (3) MinE attached to the membrane-associated MinD:ATP protein induces ATP hydrolysis: MinD:ADP, MinE, and phosphate are released into cytoplasm, (4) MinD:ADP is converted back into MinD:ATP by nucleotide exchange.

Our model, described in Ref. 20, extends the model proposed by Huang *et al.*<sup>(14)</sup> by taking into account the spatial organization of the MinD:ATP molecules on the membrane (two-stranded filaments) at the level of the single molecule. In this paper we assume that filaments are single-stranded (Fig. 1). As in the previous model, the hydrolysis rate depends on the number of bonds membrane-associated MinD:ATP has established with other membrane-associated MinD:ATP molecules. We expect that the probability for the detachment (induced by ATP hydrolysis) of the membrane-associated MinD:ATP molecule at the end of the filament (one bond established) is greater than for any other membrane-associated MinD:ATP within the filament (two bonds established). The detachment

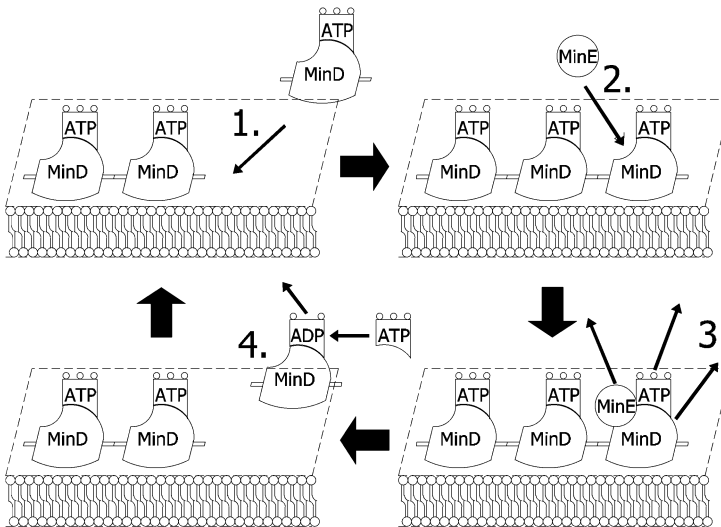


**Fig. 1.** Schematic representation of four stages in MinD/MinE proteins dynamics. (1) Cytoplasmic MinD:ATP binds to the inner layer of the cytoplasmic membrane, (2) Cytoplasmic MinE binds to the membrane-associated MinD:ATP, (3) MinE induces ATP hydrolysis, releasing subsequently MinD:ADP, MinE, and phosphate into the cytoplasm, (4) MinD:ADP is converted back into MinD:ATP by nucleotide exchange.

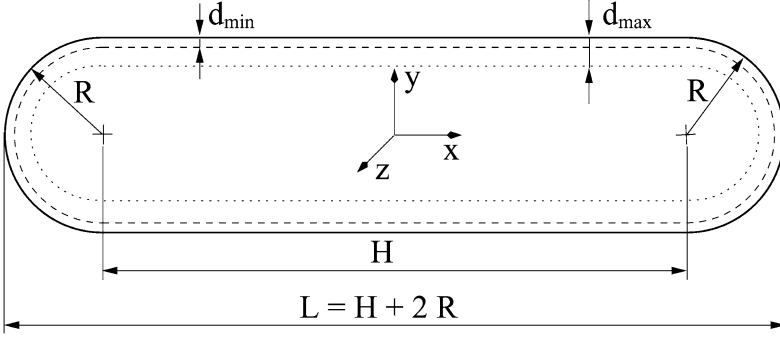


**Fig. 2.** Geometric shape used to model the bacterium *E. coli*: cylinder of length  $H$  and radius  $R$  with two hemispheres of radius  $R$  at either end. The origin of the coordinate system  $(x, y, z)$  is placed in the center of the bacterium. Two distances from the membrane,  $d_{\min}$  and  $d_{\max}$ , are used to define the region near the membrane ( $d < d_{\min}$ ) and the region far from the membrane ( $d > d_{\max}$ ), respectively. For details see text. All parameters shown in the figure are scaled equally, except the parameter  $d_{\min}$ .

probability for a membrane-associated MinD:ATP that has zero bonds established is expected to be the highest.

*E. coli* is a rod-shaped bacterium. In our model, it is approximated by a cylinder of length  $H$  and radius  $R$  with two hemispheres of radius  $R$  at either end (two poles of the bacterium), giving the total length  $L = H + 2R$  (Fig. 2). For the computational reasons (discussed later in the text), the volume bounded by the cylinder and two hemispheres is divided into three regions: the region near the membrane ( $d < d_{\min}$ ), the region far from the membrane ( $d > d_{\max}$ ), and the intermediate region ( $d_{\min} < d < d_{\max}$ ), where  $d$  denotes the distance from the membrane.

The simulation starts with the MinD:ATP and MinE proteins arbitrary distributed in the cytoplasm, where they diffuse freely. The off-lattice diffusion in the three-dimensional space is described using Smoluchowski dynamics.<sup>(22,23)</sup> A protein starts from a well-defined position  $\mathbf{r}$  at time  $t$  and diffuses during a time  $\Delta t$ . Probability density for finding a protein at time  $t + \Delta t$  at a position  $\mathbf{r} + \Delta \mathbf{r}$  is described by

$$p(\mathbf{r} + \Delta \mathbf{r}, t + \Delta t) = G_s(\Delta x)G_s(\Delta y)G_s(\Delta z), \quad (1)$$

$$G_s(\Delta x) \equiv \frac{1}{s\sqrt{2\pi}} \exp\left(-\frac{(\Delta x)^2}{2s^2}\right), \quad (2)$$

$$s \equiv \sqrt{2D\Delta t}, \quad (3)$$

where  $G_s(\Delta x)$  is a normalized Gaussian distribution with deviation  $s$  (diffusion length), and diffusion coefficient  $D$ . If the protein encounters the membrane, it will reflect from it.

The cytoplasmic MinD:ATP protein on its Brownian-journey through the cytoplasm may enter the region near the membrane ( $d < d_{\min}$ ). Only the proteins located in this region interact with the membrane, i.e. the parameter  $d_{\min}$  is used to define the interaction region.

Imagine a small box (cuboid) with height  $d_{\min}$  and a base with area  $A$  placed on the membrane. Let  $N_{d_{\min}}^{\text{cyt}}(t)$  and  $\langle \rho_{d_{\min}}^{\text{cyt}}(t) \rangle$  stand for the number of MinD:ATP found in the small box at the time  $t$ , and the average concentration of MinD:ATP in the small box at the time  $t$ , respectively. Then the number of MinD:ATP molecules that will be attached to the selected part of the membrane (the base of the cuboid) in the time interval  $\Delta t$  (denoted by  $\Delta N(t)$ ) is given by

$$\Delta N(t) \approx \sigma_D \langle \rho_{d_{\min}}^{\text{cyt}}(t) \rangle A \Delta t \approx \sigma_D \frac{N_{d_{\min}}^{\text{cyt}}}{d_{\min} A} A \Delta t, \quad (4)$$

where  $\sigma_D$  stands for the reaction rate parameter.

Since we expect (and the simulation results confirm) that the average concentration of the cytoplasmic MinD:ATP molecules in the region near the membrane only weakly depends on the parameter  $d_{\min}$ , the same is valid for the number of MinD:ATP molecules that will be attached to the membrane in the time interval  $\Delta t$ . This implies that  $d_{\min}$  is only the model (simulation) parameter used to define the region near the membrane, and should not be interpreted as a physical interaction radius.

However, the probability for the attachment of MinD:ATP to the membrane,  $p_D = \Delta N(t) / N_{d_{\min}}^{\text{cyt}}(t)$ , depends on the parameter  $d_{\min}$ :

$$p_D = \frac{\Delta N(t)}{N_{d_{\min}}^{\text{cyt}}(t)} \approx \sigma_D \frac{\Delta t}{d_{\min}}. \quad (5)$$

If the reaction takes place, MinD:ATP attaches to the nearest point on the membrane with the random orientation. (Our model forbids this reaction to take place if the position where the protein should bind is already occupied by another MinD:ATP.) This new membrane-associated MinD:ATP serves as the seed at which MinD filament may be formed. The orientation of the seed (which is random) determines the orientation of the filament that may be formed on that seed (Fig. 1).

Cytoplasmic MinD:ATP protein located in the region near the membrane interacts (in addition to the pure protein-membrane interaction) with the membrane-associated MinD:ATP proteins: cytoplasmic MinD:ATP protein try to attach to the free attachment site of the membrane-associated MinD:ATP protein. If the distance from the free attachment site to the cytoplasmic MinD:ATP protein is less than  $d_{\min}$  then the reaction can take place. In other words, the free attachment site is the center of the ‘‘binding half-sphere’’ of the radius  $r = d_{\min}$ . The probability

for this reaction to take place depends on the reaction rate parameter  $\sigma_{Dd}$ :

$$p_{Dd} = \sigma_{Dd} \frac{\Delta t}{V}; \quad V = \frac{2\pi}{3} d_{\min}^3. \quad (6)$$

The probability for the binding site to be occupied by one of the MinD:ATP proteins (located within the half-sphere) must not depend on the radius of the half-sphere. Since we assume that the average concentration of MinD:ATP proteins only weakly depends on the radius of the half-sphere, the probability for the reaction to take place is inversely proportional to the volume of the binding half-sphere.

An attachment of MinE to the membrane-associated MinD:ATP complex can take place if proteins are within the interaction radius ( $r < d_{\min}$ ) and there is no MinE protein already attached. The probability for this reaction is

$$p_E = \sigma_E \frac{\Delta t}{V}; \quad V = \frac{2\pi}{3} d_{\min}^3. \quad (7)$$

MinE protein in the membrane-associated MinE-MinD:ATP complex stimulates detachment of the complex from the membrane by inducing ATP hydrolysis. The probability for this reaction might depend on the number of bonds particular MinD:ATP has formed with its MinD:ATP neighbors, and we assume that the number of bonds established decreases the reaction probability. Let  $\sigma_{de}^{(i)}$ ,  $i = 0, 1, 2$  stand for the detachment reaction rate when the MinD protein has  $i$  bonds established. Hence,

$$\sigma_{de}^{(0)} > \sigma_{de}^{(1)} > \sigma_{de}^{(2)}, \quad (8)$$

and the probability for this reaction is:

$$p_{de}^{(i)} = 1 - \exp(-\sigma_{de}^{(i)} \Delta t) \approx \sigma_{de}^{(i)} \Delta t. \quad (9)$$

The transformation of MinD:ADP into MinD:ATP by nucleotide exchange is treated as unimolecular reaction with reaction rate  $\sigma_D^{ADP \rightarrow ATP}$ . Hence, the probability for this reaction during time interval  $\Delta t$  is

$$p_D^{ADP \rightarrow ATP} = 1 - \exp(-\sigma_D^{ADP \rightarrow ATP} \Delta t) \approx \sigma_D^{ADP \rightarrow ATP} \Delta t. \quad (10)$$

Interactions used in our simulation are ordered (one may randomize the order of interactions at the beginning of each time step). As the time step used in the simulation is small, the probability for reactions to take place is low. Hence, the order of interactions is irrelevant.

In order to speed up the simulation, an algorithm with adaptive time steps is implemented. In the region far away from the membrane only nucleotide exchange

may take place, and that reaction is modelled as unimolecular reaction. In the region near the membrane, in addition to unimolecular reactions, bimolecular reactions are taking place. For that reason, one can use longer time step in the region far away from the membrane than in the region near the membrane. For example, consider the situation in which the cytoplasmic MinD:ATP protein interacts with the free attachment site at the MinD filament formed on the membrane. The radius of the binding half-sphere,  $d_{\min}$ , defines the scale for the simulation of the Brownian motion. Hence, the time step  $\Delta t$  used for simulating the Brownian motion in the binding half-sphere must fulfill the condition  $s \equiv \sqrt{2D\Delta t} \ll d_{\min}$ . The scale for the simulation of Brownian motion in the region far away from the membrane is the dimension of the cell; hence, in that region  $s \equiv \sqrt{2D\Delta t} \ll R$ . These two regions are connected with the transitional region ( $d_{\min} < d < d_{\max}$ ). In the transitional region time step is gradually decreased as approaching the membrane. Thus we prevent that proteins entering the region near the membrane diffuse too far and avoid bimolecular reactions on their path.

### 3. RESULTS

In the numerical simulations, the parameters related to the geometry of the *E. coli* cell (Fig. 2) are fixed to  $R = 0.4 \mu\text{m}$  and  $L = 3 \mu\text{m}$ . The MinD monomer length in the single-stranded filament is fixed to 5 nm.<sup>(10)</sup> Since the MinE monomer geometry is irrelevant, it is reduced to a point.

Diffusion constants for cytoplasmic MinD and MinE proteins used in the simulation are in good agreement with the measured values for *E. coli* proteins of a similar size:<sup>(24)</sup>

$$D_D = D_E = 2.5 \mu\text{m}^2 \cdot \text{s}^{-1}. \quad (11)$$

In our model there are three hydrolysis rate parameters. They obey the following ratios:

$$\begin{aligned} \sigma_{de}^{(0)} : \sigma_{de}^{(1)} : \sigma_{de}^{(2)} &= 400 : 40 : 1 \\ \sigma_{de}^{(0)} &= 18 \text{ s}^{-1}. \end{aligned} \quad (12)$$

The simulations reveal that Min-protein oscillations (Figs. 3 and 4) may be generated only if the parameter  $\sigma_{de}^{(2)}$  is taken significantly smaller than the other two hydrolysis rate parameters:

$$\sigma_{de}^{(2)} \ll \sigma_{de}^{(1)}, \sigma_{de}^{(0)}. \quad (13)$$

This prediction of our model has not been experimentally tested yet.

The remaining reaction rate parameters are similar to those we have used in our previous paper with two-stranded MinD filaments<sup>(20)</sup> and to those Huang

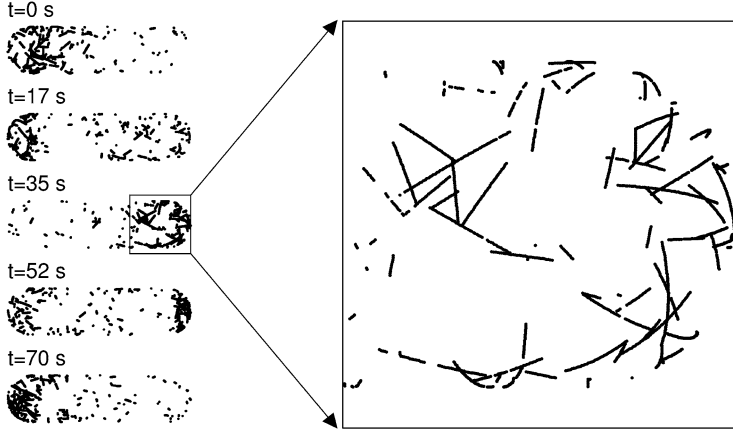


**Fig. 3.** Orthogonal projection of the membrane-associated MinD proteins onto a plane parallel to the line connecting two poles of the bacterium. Each projected protein is represented with a dot. Five time frames are shown. They refer to times  $0, \frac{1}{4}T, \frac{2}{4}T, \frac{3}{4}T, T$ ; where  $T \approx 70$  s is the period of oscillation obtained with parameters specified in the text.

*et al.*<sup>(14)</sup> have used in their analytical model:

$$\begin{aligned} \sigma_D &= 0.03 \mu\text{m} \cdot \text{s}^{-1}, \quad \sigma_{Dd} = 0.02 \mu\text{m}^3 \cdot \text{s}^{-1}, \\ \sigma_E &= 0.5 \mu\text{m}^3 \cdot \text{s}^{-1}, \quad \sigma_D^{ADP \rightarrow ATP} = 1.0 \text{s}^{-1}. \end{aligned} \quad (14)$$

In our simulation we use 3000 MinD proteins and 1050 MinE homodimers, in order to preserve concentration measured in *in vitro* experiment.<sup>(25)</sup> The simulation is evolved in time with the time step  $\Delta t = 5.5 \times 10^{-5}$  s in the region far away from the membrane ( $d > d_{\max} = 0.1 \mu\text{m}$ ), and  $\Delta t = 5.5 \times 10^{-7}$  s in the region near the membrane ( $d < d_{\min} = 0.01 \mu\text{m}$ ). In the transitional region time steps are gradually decreased as approaching the membrane.

The output of our simulation is presented in the Figs. 3 and 4. MinD and MinE pole-to-pole oscillations are generated using the parameter set given in the text above. The portion of the Fig. 3 is enlarged so that the size of the MinD single-stranded filaments formed on the membrane could be visible. In the Fig. 4 several experimentally observed phenomena are reproduced: dynamic MinD polar cup (thick dark region in the left graph), oscillating MinE ring (thin dark region in the right graph), and weakly fluorescent, rapidly moving MinE ring (the region in the right graph marked with an ellipse). Notice that (i) as the MinD polar cup shrinks and disappear at one pole, the new polar cup is forming near the center of the cell, (ii) the MinE ring moves towards one pole, disappear, reappear near



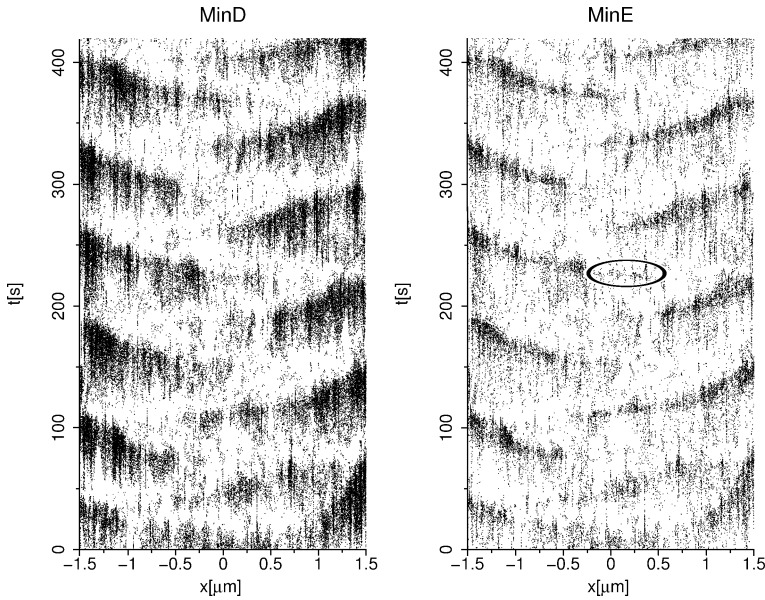


**Fig. 4.** Space-time plot for the membrane-associated MinD (left graph) and MinE proteins (right graph). Each protein is represented with a small black dot. Only 10% of all membrane-associated proteins are plotted in order to get a clear enough figure; plotted proteins are randomly chosen. In the MinE graph, weakly fluorescent and rapidly moving MinE ring is marked with an ellipse. Parameters used to obtain this figure are the same as the parameters used in the Fig. 3. Initially, all MinD and MinE are placed in the center of *E. coli*. The oscillation starts after a transient period which lasts less than one oscillation cycle (approximately 50 seconds).

the center and moves toward the other pole. Both results are in accordance with experiments.

We have additionally tested our model by applying it to the filamentous cells. Only the cell length and the number of MinD and MinE were modified:  $L = 8 \mu\text{m}$ , the number of MinD equals 8000, and the number of MinE equals 2800. The concentration of MinD and MinE is kept the same as in the simulations for cells with  $L = 3 \mu\text{m}$ . Results are shown in the Fig. 5. We have initially placed all MinD and MinE near the pole of the cell in order to put the system far away from the oscillation doubling pattern. Despite the initial condition, this pattern appeared. It is periodically interchanged with other not so symmetrical patterns. Zebra-striped patterns are also clearly visible.

As in our previous paper,<sup>(20)</sup> we have verified that oscillation patterns do not depend on the initial distribution of MinD:ATP and MinE proteins (many different initial distributions were tried). In this paper, we have additionally examined the effect the simulation parameters  $d_{\text{min}}$  and  $\Delta t$  have on the simulation output.

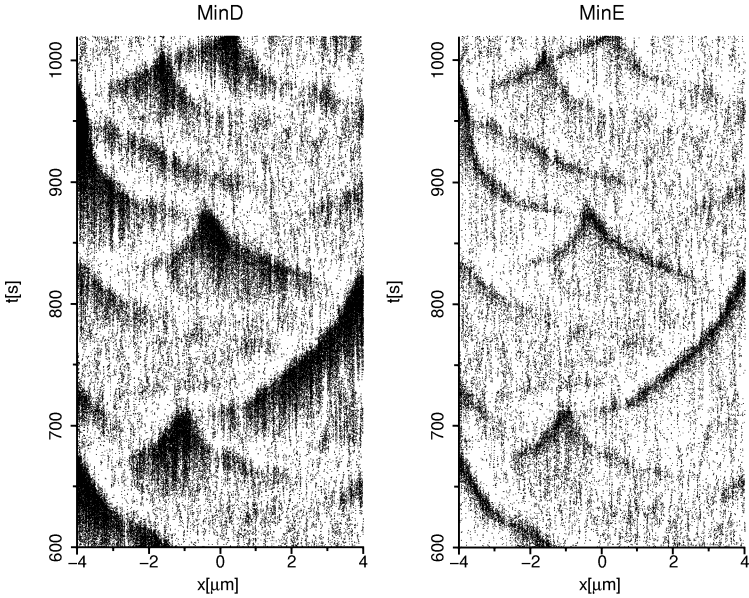


**Fig. 5.** Space-time plot for the membrane-associated MinD (left graph) and MinE proteins (right graph) in the filamentous cell ( $L = 8 \mu\text{m}$ ). Each protein is represented with a small black dot. Only 5% of all membrane-associated proteins are plotted in order to get a clear enough figure; plotted proteins are randomly chosen. Parameters used to obtain this figure are the same as the parameters used in the Figs. 3 and 4 except:  $L = 8 \mu\text{m}$ , the number of MinD equals 8000, and the number of MinE equals 2800. Initially, all MinD and MinE are placed near the pole of *E. coli*. The transient period is not shown.

The simulations have been performed with the substantially different sets of the parameters  $d_{\min}$  and  $\Delta t$ . The parameter  $d_{\min}$  fulfills the conditions:  $d_{\min}, d_{\max} \ll R$ , and  $s \ll d_{\min}$ . The mean value of the x-coordinate of the membrane-associated MinD proteins as a function of time for three sets of the simulation parameters is shown in Fig. 6a and 6b. The shapes and the periods of oscillation of the variable  $\bar{x}$  are similar despite the fact that sets of the simulation parameters differ substantially. In the Fig. 6c both plots correspond to the same set of parameters and are obtained in the same computer run. The plots differ because they are translated in time with respect to one another. The small differences are the result of stochastic effects. When the physical parameter is changed, the differences becomes more pronounced (Fig. 6d).

#### 4. COMPARISON WITH OTHER STOCHASTIC MODELS

Several stochastic models have been built to account for Min protein oscillations.<sup>(18–21)</sup> Each of these models requires a subtle ingredient in order to

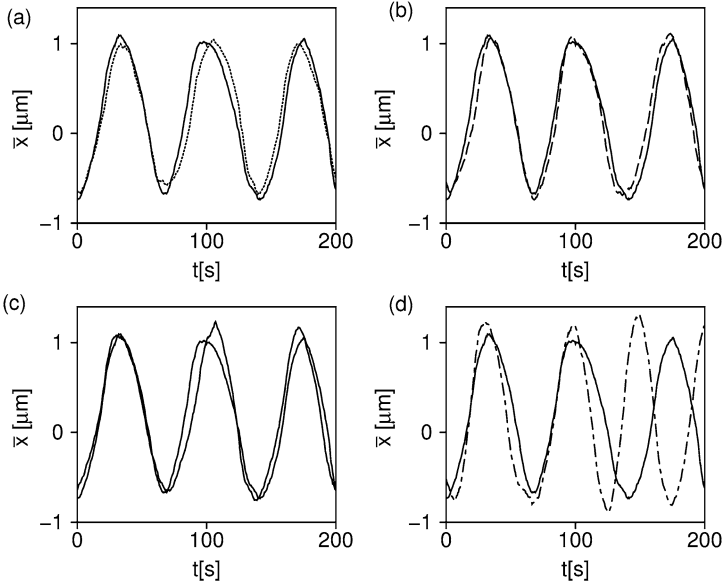


**Fig. 6.** Mean value of the  $x$ -coordinate ( $\bar{x} = \frac{1}{N} \sum_{i=1}^N x_i$ ) of the membrane-associated MinD proteins as a function of time for four sets of two simulation parameters— $d_{\min}$  and  $\Delta t$ . Values of these simulation parameters are given in Table 1. All the remaining parameters are fixed at values used to obtain results in Fig. 3. Only in (d) the physical parameter  $\sigma_{Dd}$  is changed.

produce Min oscillations. In the one-dimensional model proposed by Howard and Rutenberg, oscillations are produced only if MinE is driven onto the membrane by cytoplasmic MinD.<sup>(18)</sup> However, experiments suggest that MinE is recruited to the membrane by membrane-associated MinD.<sup>(8)</sup> In the three-dimensional model

**Table 1.** Three sets of values for two simulation parameters ( $d_{\min}$ ,  $\Delta t$ ) used to obtain results in Fig. 6

| $d_{\min}$ ( $\mu\text{m}$ ) | Region near the membrane |                | $\sigma_{Dd}$ ( $\mu\text{m}^3 \text{s}^{-1}$ ) | Region far from the membrane |                | Intermediate region  |      |
|------------------------------|--------------------------|----------------|---|------------------------------|----------------|----------------------|------|
|                              | $s/d_{\min}$             | $\Delta t$ (s) |   | $s/d_{\max}$                 | $\Delta t$ (s) |                      |      |
| —                            | 0.05                     | 1/6            | $1.4 \times 10^{-5}$                            | 0.02                         | 1/6            | $5.5 \times 10^{-5}$ | 1/6  |
| ...                          | 0.01                     | 1/6            | $5.5 \times 10^{-7}$                            | 0.02                         | 1/6            | $5.5 \times 10^{-5}$ | 1/6  |
| --                           | 0.05                     | 1/20           | $1.25 \times 10^{-6}$                           | 0.02                         | 1/20           | $5.0 \times 10^{-6}$ | 1/20 |
| ---                          | 0.05                     | 1/6            | $1.4 \times 10^{-5}$                            | 0.01                         | 1/6            | $5.5 \times 10^{-5}$ | 1/6  |

*Note.* The diffusion length ( $s \equiv \sqrt{2D\Delta t}$ ) is given for the sake of clarity, and the parameter  $d_{\max}$  is fixed to  $0.1 \mu\text{m}$ . The fourth set differs from the first one in only one parameter— $\sigma_{Dd}$ .

proposed by Kerr *et al.*,<sup>(19)</sup> when the reaction between the cytoplasmic MinD:ATP and the membrane-associated MinD take place, the cytoplasmic MinD:ATP will attach to the membrane at a free place that is located within the unphysically large “search radius” (50–100 nm). Tostevin and Howard developed an one-dimensional on-lattice model.<sup>(21)</sup> To produce oscillations they assume that cytoplasmic MinD:ATP attaches to the membrane-associated MinD:ATP cooperatively, and to the membrane-associated MinE-MinD:ATP complex isodesmically. In other words, the reaction rate for attaching the cytoplasmic MinD:ATP to the membrane-associated MinD:ATP is substantially higher than the reaction rate for attaching it to the membrane-associated MinE-MinD:ATP complex. In our three-dimensional off-lattice stochastic model, oscillations are produced only if the hydrolysis rates are taken to strongly depend on the number of bonds membrane-associated MinD proteins have established with other membrane-associated MinD proteins: up to three bonds in the two-stranded filaments,<sup>(20)</sup> and up to two two bonds in the single-stranded filaments (the model presented in this article).

In our opinion, physically acceptable assumptions are only the assumption Tostevin and Howard have introduced and our assumption. However, since the model proposed by Tostevin and Howard is one-dimensional, we have adapted our software to additionally test their model (their assumption) in the three-dimensional environment. The majority of their parameters map directly into our set of parameters:  $L = 3 \mu\text{m}$ ,  $D_D = D_E = 2.0 \mu\text{m}^2 \cdot \text{s}^{-1}$ ,  $\sigma_{de}^{(0)} = 10 \text{s}^{-1}$ ,  $\sigma_{de}^{(0)} : \sigma_{de}^{(1)} : \sigma_{de}^{(2)} = 100 : 3 : 1$ , the number of MinD equals 3000, and the number of MinE homodimers equals 1200. The remaining parameters used in their stochastic on-lattice simulation ( $\sigma_{d,sp} = 0.001 \text{s}^{-1}$ ,  $\sigma_{d,coop} = 30 \text{s}^{-1}$ ,  $\sigma_e = 50 \text{s}^{-1}$ ) are simply related to the corresponding parameters in our three-dimensional off-lattice simulation ( $\sigma_D$ ,  $\sigma_{Dd}$ ,  $\sigma_E$ ):

$$\sigma_D \approx \frac{R}{2} \sigma_{d,sp} = 0.001 \mu\text{m} \cdot \text{s}^{-1}, \quad (15)$$

$$\sigma_{Dd} \approx R^2 \pi (\Delta x) \sigma_{d,coop} = 0.15 \mu\text{m}^3 \cdot \text{s}^{-1} \quad (16)$$

$$\sigma_E \approx R^2 \pi (\Delta x) \sigma_e = 0.25 \mu\text{m}^3 \cdot \text{s}^{-1}, \quad (17)$$

where  $\Delta x = 0.01 \mu\text{m}$  is the distance between neighboring nodes of the lattice, and  $R = 0.4 \mu\text{m}$ . Let us derive the relation between these two sets of parameters. Imagine a cylinder of length  $L$  and radius  $R$ . Divide it into the number of small cylinder each having the length  $\Delta x$ . Take one MinD protein and calculate the probability for attaching it to the membrane. This probability is equal to the product of  $p_D$  (5) and the probability for MinD to be found the region near the membrane:

$$\sigma_D \frac{\Delta t}{d_{\min}} \cdot \frac{2R\pi d_{\min} \Delta x}{R^2 \pi \Delta x} = \sigma_D \frac{2}{R} \Delta t \quad (18)$$

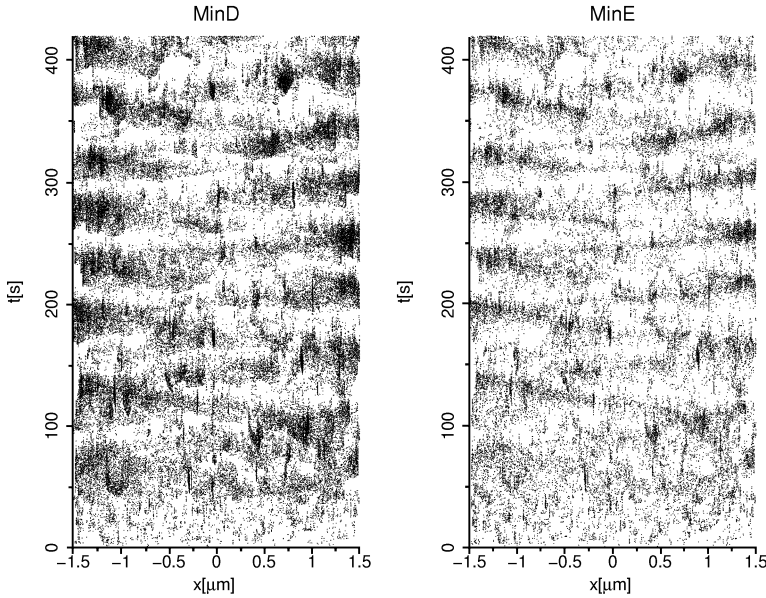


**Fig. 7.** Space-time plot for the membrane-associated MinD (left graph) and MinE proteins (right graph). Each protein is represented with a small black dot. Only 10% of all membrane-associated proteins are plotted in order to get a clear enough figure; plotted proteins are randomly chosen. Simulation parameters correspond to the parameters Tostevin and Howard used in their one-dimensional simulation.<sup>(21)</sup> Initially, all MinD and MinE are placed in the center of *E. coli*.

The same probability in the model proposed by Tostevin and Howard is given by:

$$\sigma_{d,sp} \Delta t \quad (19)$$

Equation (15) follows from Eqs. (18) and (19). Using a similar line of arguments one can derive Eqs. (16) and (17).

The simulation results are shown in the in the Fig. 7 ( $L = 3 \mu\text{m}$ ) and Fig. 8 ( $L = 8 \mu\text{m}$ ). MinD and MinE oscillations appear in both cases. However, they are not completely in accordance with experiments: Min proteins move from pole-to-pole more or less continuously. MinD filaments (data not shown) are approximately five times longer than those obtained in our model (Fig. 3). We believe that the continuous Min pole-to-pole oscillations are the effect of long MinD filaments, since we have noticed the similar effect in our model when different parameter set is used which produces longer filaments. One is looking for longer filaments because of experimentally observed helices which extend between the two cell poles.<sup>(26)</sup> Our simulations suggest that those helices might be composed of many short filaments. Finally, we admit that we did not explore the parameter space of the Tostevin and Howard model, and maybe one can find the “better” parameter set.

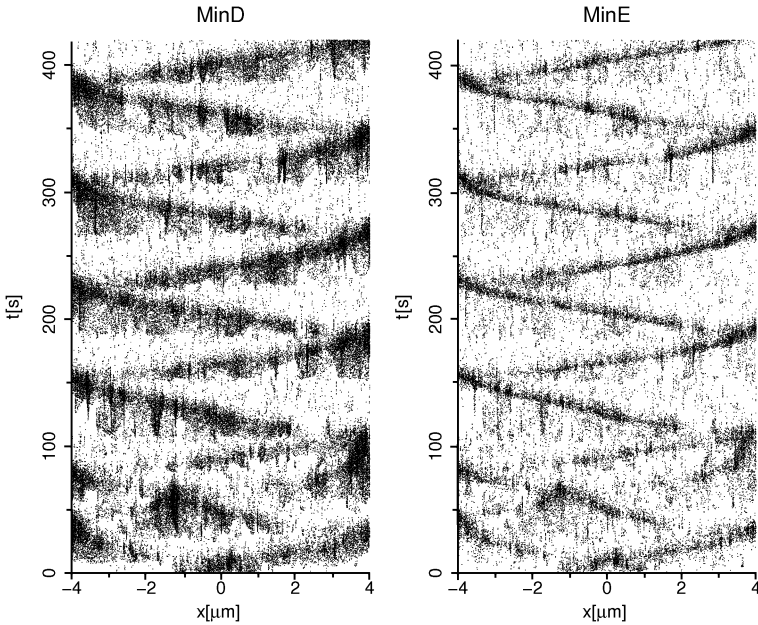


**Fig. 8.** Space-time plot for the membrane-associated MinD (left graph) and MinE proteins (right graph) in the filamentous cell ( $L = 8 \mu\text{m}$ ). Each protein is represented with a small black dot. Only 5% of all membrane-associated proteins are plotted in order to get a clear enough figure; plotted proteins are randomly chosen. Parameters used to obtain this figure are the same as the parameters used in the Fig. 7 except:  $L = 8 \mu\text{m}$ , the number of MinD equals 8000, and the number of MinE equals 3200. Initially, all MinD and MinE are placed in the center of *E. coli*.

## 5. CONCLUSION

We find that our model generates Min oscillations regardless of the MinD filaments type (single-stranded or two-stranded assumption) formed on the membrane. In both assumptions, Min-proteins oscillations appear only if the hydrolysis rate parameter (hydrolysis is induced by MinE) for the MinE-MinD:ATP protein complex with the maximum number of bonds established is taken significantly smaller than the hydrolysis rate parameter for the MinE-MinD:ATP protein complex with the less bonds established.

We have shown that the simulation output only weakly depends on the simulation parameter  $d_{\text{min}}$ . Hence, this parameter should not be interpreted as the physical interaction radius. It is only the simulation interaction radius.

Our model is a step forward in the description of the experimentally observed helices.<sup>(26)</sup> However, the filaments we have obtained with our model are not long enough. One should introduce diffusion on the membrane and lateral filament-filament interaction in order to obtain longer filaments.

## ACKNOWLEDGMENTS

We thank Ivana Šarić for a technical support, and Goran Mitrović for carefully reading our manuscript.

## REFERENCES

1. J. Lutkenhaus, Dynamic proteins in bacteria. *Curr. Opin. Microbiol.* **5**:548–552 (2002).
2. X. C. Yu and W. Margolin, FtsZ ring clusters in *min* and partition mutants: role of both the Min system and the nucleoid in regulating FtsZ ring localization. *Mol. Microbiol.* **32**:315–326 (1999).
3. P. A. J. de Boer, R. E. Crossley, and L. I. Rothfield, A division inhibitor and a topological specificity factor coded for by the minicell locus determine proper placement of the division septum in *E. coli*. *Cell* **56**:641–649 (1989).
4. E. Bi and J. Lutkenhaus, Cell division inhibitors SulA and MinCD prevent formation of the FtsZ ring. *J. Bacteriol.* **175**:1118–1125 (1993).
5. D. M. Raskin and P. A. J. de Boer, Rapid pole-to-pole oscillation of a protein required for directing division to the middle of *Escherichia coli*. *Proc. Natl. Acad. Sci. USA* **96**:4971–4976 (1999).
6. Z. Hu, A. Mukherjee, S. Pichoff, and J. Lutkenhaus, The MinC component of the division site selection system in *Escherichia coli* interacts with FtsZ to prevent polymerization. *Proc. Natl. Acad. Sci. USA* **96**:14819–14824 (1999).
7. D. M. Raskin and P. A. J. de Boer, MinDE-dependent pole-to-pole oscillation of division inhibitor MinC in *Escherichia coli*. *J. Bacteriol.* **181**:6419–6424 (1999).
8. Z. Hu, E. P. Gogol, and J. Lutkenhaus, Dynamic assembly of MinD on phospholipid vesicles regulated by ATP and MinE. *Proc. Natl. Acad. Sci. USA* **99**:6761–6766 (2002).
9. C. A. Hale, H. Meinhardt, and P. A. J. de Boer, Dynamic localization cycle of the cell division regulator MinE in *Escherichia coli*. *EMBO J.* **20**:1563–1572 (2001).
10. K. Suefuiji, R. Valluzzi, and D. RayChaudhuri, Dynamic assembly of MinD into filament bundles modulated by ATP, phospholipids, and MinE. *Proc. Natl. Acad. Sci. USA* **99**:16776–16781 (2002).
11. H. Meinhardt and P. A. J. de Boer, Pattern formation in *Escherichia coli*: A model for the pole-to-pole oscillations of Min proteins and the localization of the division site. *Proc. Nat. Acad. Sci. USA* **98**:14202–14207 (2001).
12. M. Howard, A. D. Rutenberg, and S. de Vet, Dynamic compartmentalization of bacteria: Accurate division in *E. coli*. *Phys. Rev. Lett.* **87**:278102 (2001).
13. K. Kruse, A dynamic model for determining the middle of *Escherichia coli*. *Biophys. J.* **82**:618–627 (2002).
14. K. C. Huang, Y. Meir, and N. S. Wingreen, Dynamic structures in *Escherichia coli*: Spontaneous formation of MinE rings and MinD polar zones. *Proc. Natl. Acad. Sci. USA* **100**:12724–12728 (2003).
15. R. V. Kulkarni, K. C. Huang, M. Kloster, and N. S. Wingreen, Pattern formation within *Escherichia coli*: Diffusion, membrane attachment, and self-interaction of MinD molecules. *Phys. Rev. Lett.* **93**:228103 (2004).
16. G. Mcacci and K. Kruse, Min-oscillations in *Escherichia coli* induced by interactions of membrane-bound proteins. *Phys. Biol.* **2**:89–97 (2005).
17. D. A. Drew, M. J. Osborn, and L. I. Rothfield, A polymerization-depolymerization model that accurately generates the self-sustained oscillatory system involved in bacterial division site placement. *Proc. Nat. Acad. Sci. USA* **102**:6114–6118 (2005).
18. M. Howard and A. D. Rutenberg, Pattern formation inside bacteria: Fluctuations due to the low copy number of proteins. *Phys. Rev. Lett.* **90**:128102 (2003).

19. R. A. Kerr, H. Levine, T. J. Sejnowski, and W.-J. Rappel, Division accuracy in a stochastic model of Min oscillations in *Escherichia coli*. *Proc. Nat. Acad. Sci. USA* **103**:347–352 (2006).
20. N. Pavin, H. Čipčić Paljetak, and V. Krstić, Min-protein oscillations in *Escherichia coli* with spontaneous formation of two-stranded filaments in a three-dimensional stochastic reaction-diffusion model. *Phys. Rev. E* **73**:021904 (2006).
21. F. Tostevin and M. Howard, A stochastic model of Min oscillations in *Escherichia coli* and Min protein segregation during cell division. *Phys. Biol.* **3**:1–12 (2006).
22. M. von Smoluchowski, Versuch einer mathematischen Theorie der Koagulationskinetik kolloider Lsungen. *Z. Phys. Chem., Stoechiom. Verwandtschaftsl.* **92**:129-168 (1917).
23. S. S. Andrews and D. Bray, Stochastic simulation of chemical reactions with spatial resolution and single molecule detail. *Phys. Biol.* **1**:137–151 (2004).
24. M. B. Elowitz *et al.*, Protein mobility in the cytoplasm of *Escherichia coli*, *J. Bacteriol.* **181**:197–203 (1999).
25. Y.-L. Shih *et al.*, Division site placement in *E. coli*: mutations that prevent formation of the MinE ring lead to loss of the normal midcell arrest of growth of polar MinD membrane domains. *EMBO J.* **21**:3347–3357 (2002).
26. Y.-L. Shih, T. Le, and L. Rothfield, Division site selection in *Escherichia coli* involves dynamic redistribution of Min proteins within coiled structures that extend between the two cell poles. *Proc. Natl. Acad. Sci. USA* **100**:7865–7870 (2003).